*Advances in Engineering Materials, Structures and Systems: Innovations, Mechanics and Applications – Zingoni (Ed.)*
*© 2019 Taylor & Francis Group, London, ISBN 978-1-138-38696-9*

# Shear behavior of reinforced concrete beams with GFRP needles as coarse aggregate partial replacement: Full-scale experiments

X.F. Nie
*Department of Civil and Environmental Engineering, The Hong Kong Polytechnic University, Hong Kong, China*

B. Fu
*School of Civil and Transportation Engineering, Guangdong University of Technology, Guangzhou, China*

J.G. Teng
*Department of Civil and Environmental Engineering, The Hong Kong Polytechnic University, Hong Kong, China*
*Department of Ocean Science and Engineering, Southern University of Science and Technology, Shenzhen, China*

L.C. Bank & Y. Tian
*Civil Engineering Department, City College of New York, New York, NY, USA*

ABSTRACT: Fiber reinforced polymer (FRP) waste is becoming an environmental concern due to the widespread use and non-biodegradable nature of FRP composites. Cutting FRP waste into discrete reinforcements (referred to as "needles" hereafter) as coarse aggregate in concrete has been suggested as a possible solution to FRP waste recycling. It has previously been observed in small specimens that FRP needles increase the tensile strength and energy absorption capacity of concrete. This paper presents an experimental investigation into the effect of GFRP needles as coarse aggregate partial replacement in concrete on shear behavior of full-scale reinforced concrete (RC) beams. A total of 10 RC beams without steel stirrups in the critical zone were tested under four-point bending. The volume replacement ratio of the coarse aggregate and the surface type of GFRP needles were chosen as the test parameters. GFRP needles, with either smooth or helically wrapped surfaces, were added to the concrete mix to replace 5% or 10% of coarse aggregate by volume, respectively. All test beams failed in shear in a brittle manner with the ductility being slightly enhanced by the partial replacement of coarse aggregate using GFRP needles. An enhancement of 8%-10% in the load carrying capacity was observed in beams with helically wrapped needles, while beams with smooth needles showed a reduction in the load carrying capacity.

## 1 INTRODUCTION

Fiber-reinforced polymer (FRP) composite materials have been extensively and increasingly used in various industries, such as aerospace, marine and construction, for over half a century (Yazdanbakhsh and Bank 2014). An increasing number of FRP vessels, wind turbines and structural components are approaching the end of their service or functional lives, leading to an increasing rate of FRP waste accumulation (Yazdanbakhsh and Bank 2014). Due to the widespread use and non-biodegradable nature of FRP composites, FRP waste is becoming an environmental concern. Cutting FRP waste into discrete reinforcements (referred to as "needles" hereafter) as coarse aggregate in concrete may be a possible solution for this issue (Yazdanbakhsh et al. 2017, 2018; Dong et al. 2019). Yazdanbakhsh et al. (2017) have conducted an experimental study on the mechanical properties of concrete with coarse aggregate partially replaced by FRP needles which were produced by cutting GFRP reinforcing bars. It was found from their study that due to the presence of FRP needles, even though the compressive strength of concrete reduced slightly by 5-9%, the splitting tensile strength of the concrete increased by 22-33%. Moreover, post-failure toughness of the concrete in both compression and tension was significantly increased as a result of the incorporation of FRP needles.

To verify the effectiveness of needle reinforced concrete to enhance the structural performance of full-scale structural members, this paper presents an experimental investigation into the effect of GFRP needles as coarse aggregate partial replacement in concrete on the shear behavior of reinforced concrete (RC) beams. The GFRP needles as part of the coarse aggregate were expected to enhance the shear strength and ductility of the RC beam as they (1) directly contribute to the shear strength, which is similar to steel stirrups;

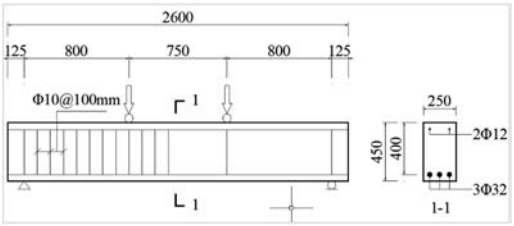


Figure 1. Details of the test specimens (dimensions in mm).

and (2) limit the development of shear or flexural-shear cracks, thus improving aggregate interlock and dowel action of flexural reinforcement.

## 2 EXPERIMENTAL PROGRAM

### 2.1 *Specimen details*

Ten full-scale beam specimens with cross-sections of 250 mm × 450 mm and a length of 2,600 mm were tested. The details of the test specimens are shown in Fig. 1. Two steel bars of 12 mm diameter were used as top support bars in the compression zone, and three steel bars of 32 mm diameter were used as the primary tension reinforcements. Four stirrups, which were formed from smooth steel bars of a small diameter (10 mm), were used to facilitate the fabrication of steel cages. These four stirrups were located at the two supports and two loading points, where shear cracks do not occur, and the presence of these stirrups was expected to have a negligible effect on the shear behaviour of the specimens. Stirrups of 10 mm diameter at a spacing of 100 mm were provided in the left half of the beam so that the shear capacity of the left shear span was much larger than that of the right shear span. Such an arrangement of stirrups was to ensure that the shear failure of the beam would occur in the right shear span The concrete cover (from beam soffit to the outer surface of steel tension bars) was 34 mm, leading to an effective height of 400 mm for the test specimen. The shear span ratio (λ) (i.e., length of shear span/effective height) adopted in this study was 2.0, providing a length of shear span of 800 mm.

The test parameters examined in this study were the volume replacement ratio of coarse aggregate ($v_n$) and the surface type of GFRP needles. FRP rebar needles were incorporated in concrete to replace 0%, 5% and 10% of coarse aggregate by volume. Smooth pultruded GFRP rods or helically wrapped GFRP rebars were used to produce needles, in order to study the effect of the bond between the FRP needles and concrete on the behavior of the beams. In the present study, GFRP rods/rebars of 6 mm in diameter were cut into needles of 100 mm in length (as shown in Fig. 2), which was the length used in tests by Yazdanbakhsh et al. (2017).

The ten test specimens were divided into 5 pairs. Each pair included two identical beams. Detailed arrangement of the test specimens is given in Table 1, in which each specimen is designated a name. Each


Figure 2. GFRP needles cut from FRP rods/rebars and used in the study.

Table 1. Specimen arrangement.

| Group | Specimen name | $v_n$ (%) | Surface type of needles |
|---|---|---|---|
| 1 | V0SMa | 0 | – |
| | V0SMb | 0 | – |
| 2 | V5SMa | 5 | Smooth |
| | V5SMb | 5 | Smooth |
| 3 | V10SMa | 10 | Smooth |
| | V10SMb | 10 | Smooth |
| 4 | V5HWa | 5 | Helically wrapped |
| | V5HWb | 5 | Helically wrapped |
| 5 | V10HWa | 10 | Helically wrapped |
| | V10HWb | 10 | Helically wrapped |

specimen name consists of three sets: “V0”, “V5” and “V10” in the first letter-number combination represents the volume replacement ratios of coarse aggregate of 0%, 5% and 10% respectively; the second letter sets of “SM” and “HW” stand for smooth needles and helically wrapped needles respectively; and the last letter “a” and “b” represent two samples of a beam with the same parameters. For example, Specimen V5SMa is the first identical beam in which the volume replacement ratio of coarse aggregate using smooth GFRP needles is 5%.

### 2.2 *Material properties*

Standard tensile tests according to BS-18 (BSI 1987) were conducted to determine the material properties of steel bars used in the study. For each kind of steel bar, three specimens were tested. The averaged yield stress, ultimate stress and elastic modulus of steel bars are listed in Table 2.

The smooth pultruded GFRP rods and helically wrapped GFRP rebars used in this study were both produced by the same company and made from the same glass fiber and resin (unsaturated polyester resin).

Table 2. Material properties of steel bars and GFRP rods/bars.

| Properties | Steel bars of 12 mm in diameter | Steel bars of 32 mm in diameter | Smooth pultruded rods | Helically wrapped rebars |
|---|---|---|---|---|
| Yield stress (MPa) | 381.6 | 459.9 | | |
| Ultimate stress (MPa) | 504.5 | 633.3 | 620.2 | 1147.6 |
| Elastic modulus (GPa) | 190.1 | 192.9 | 39.4 | 62.7 |
| Mass fraction of fiber (%) | | | 69.5 | 78.7 |
| Volume fraction of fiber (%) | | | 50.1 | 62.0 |

Table 3. Strength of small specimens with needles (MPa).

| Group | Corresponding beam specimen | Flexural strength of small beams | Splitting tensile strength of cylinders | Compressive strength of cylinders |
|---|---|---|---|---|
| 1 | V0SMa<br>V0SMb | 4.29 | 3.60 | 40.5 |
| 2 | V5SMa<br>V5SMb | 5.12 | 4.07 | 50.1 |
| 3 | V10SMa<br>V10SMb | 6.36 | 4.42 | 42.9 |
| 4 | V5HWa<br>V5HWb | 3.97 | 3.43 | 36.9 |
| 5 | V10HWa<br>V10HWb | 4.69 | 3.70 | 35.4 |

Standard tensile tests according to ASTM D7205 (ASTM 2011) were conducted to determine the material properties of GFRP bars/rods used in the study. For each kind of GFRP bar/rod, five specimens were tested. The averaged ultimate stress and elastic modulus of GFRP bars/rods are listed in Table 2. Burn-out tests were conducted according to ASTM D2584 (ASTM 2018b) to determine the mass and volume fractions of fiber for the smooth and helically wrapped GFRP needles. For each kind of needle, five specimens were tested. The averaged burn-out test results are also listed in Table 2.

For each group of concrete, three small beams with the dimensions of 150 mm in width and depth × 550 mm in length were tested following ASTM C1609 (ASTM 2012) to obtain their flexural strength, and three cylinder specimens with the dimensions of 150 mm in diameter × 300 mm in height were tested following ASTM C496 (ASTM 2017) to obtain their splitting tensile strength, and another three cylinder specimens were tested following ASTM C39 (ASTM 2018a) to obtain their compressive strength. The measured material properties of the five groups of concrete are listed in Table 3. It can be seen from Table 3 that with coarse aggregate replacement by smooth needles at either 5% (Group 2) or 10% (Group 3) in volume, the flexural strength of small beams, splitting tensile strength of cylinders and compressive strength of cylinders are all larger than those of the control specimens (Group 1); with coarse aggregate replacement by helically wrapped needles at 5% (Group 4) in volume, the flexural strength of small beams, splitting tensile strength of cylinders and compressive strength of cylinders are all smaller than those of the control specimens; and with coarse aggregate replacement by helically wrapped needles at 10% (Group 5) in volume, the compressive strength of cylinders is smaller than that of the control specimens, but the flexural strength of small beams and splitting tensile strength of cylinders are larger than those of the control specimens. Moreover, it can be seen that with a larger volume of coarse aggregate replaced with either smooth needles or helically wrapped needles, the flexural strength of small beams and splitting tensile strength of cylinders are larger, while the compressive strength of cylinders is smaller It should be noted that the splitting tensile strength results of cylinders with the helically wrapped needles do not agree with observations made by Yazdanbakhsh et al. (2017). This may be due to the differences in the helically wrapped needles used in the two tests. The helically wrapped needles used in Yazdanbakhsh et al. (2017) were sand coated while those used in the present study were not. Five LVDTs were used to measure deflections - one at each support, one at each loading point and one at the beam midspan. Two strain gauges of 80 mm in gauge length were attached to the compression face of the mid-span of the specimens to measure the strain of the compressive concrete. One strain gauge of 5 mm in gauge length was installed onto one side of each tension steel bar at mid-span to measure the strains of tension steel bars. Detailed data from these gauges will be presented elsewhere.

Figure 3. Test set-up of beam specimens.

The test set-up of the beam specimens is shown in Fig. 3. Four-point bending was used for testing all the beam specimens. The loads were applied through two hydraulic jacks, which were connected to a single manually-operated pump, to ensure equal loading for the two jacks. A load cell was installed under each loading point to measure the precise load from the loading

(a) Crack Pattern I (b) Crack Pattern II

Figure 4. Failure modes of the beam specimens.

(a) V10SMb (b) V10HWb

Figure 5. The distribution and condition of the needles along the main shear crack.

point. The loading was operated using a manual jack, and the loading rate was quasi-static The typical time taken to complete each test was about 4 hours. A data acquisition system capable of digitally recording and storing load, deflection and strain data at a sampling frequency of 1 Hz was used in the test.

## 3 FAILURE MODES

All ten beams failed by shear due to the formation of a main diagonal crack in the right shear span (the shear span without stirrups) which linked the right loading point and right support. The failure of all ten beams was abrupt, with different levels of noise made by beams with different volumes of FRP needles. The two control beams (V0SMa and V0SMb) made a very loud noise when they failed, while the four beams with 10% of coarse aggregate in volume replaced by FRP needles (V10SMa, V10SMb, V10HWa and V10HWb) made very little noise when they failed; the noise made by the four beams with 5% of coarse aggregate in volume replaced by FRP needles (V5SMa, V5SMb, V5HWa and V5HWb) when they failed was less than that made by the two control beams but more than that made by the four beams with 10% of coarse aggregate in volume replaced by FRP needles. The loading was not stopped when the beams failed, but was continued until the deflection was large enough or the loading header was out of perpendicular alignment; it would be dangerous if the loading was still continued. It should be noted that even though all ten beams failed by shear, two kinds of crack patterns were seen (as shown in Fig. 4): (1) Crack Pattern I: the main diagonal crack was at about 45 degrees to the horizontal line. The 45-degree crack extended from the loading point to the top of the main rebars. It then extended along the top of the rebars to the right support (the crack pattern shown in Fig. 4a); and (2) Crack Pattern II: the main diagonal crack was at approximately 30 degrees to the horizontal and extended from the loading point directly to the right support (the crack pattern shown in Fig. 4b). Only two of the ten beams exhibited Crack Pattern II (V5SMb and V10HWa) while the other eight beams all exhibited Crack Pattern I. This situation that two beams in the same group (e.g. V5SMa and V5SMb) exhibited different crack patterns may be due to the natural variability of reinforced concrete specimens, which is known to be especially significant when testing concrete beams in shear.

After the testing, the ends of the failed beam specimens with needles were broken off along the main shear cracks to see the distribution and condition of the needles, as shown in Fig. 5, in which Specimens V10SMb and V10HWb were taken as examples. It can be seen from Fig. 5 that the vast majority of the needles across the main shear crack were pulled out of the concrete. It can also be seen that the helically wrapped needles are more firmly and more deeply embedded in the concrete. Most of these needles were undamaged, and rupture of the needles was rarely observed.

## 4 LOAD-DEFLECTION RESPONSES OF BEAMS

### 4.1 *Load-deflection curves*

The load-deflection curves of the ten test specimens are shown in Fig. 6, in which the vertical axis shows the shear force (half of the total beam load, averaged from the forces of the two load cells) and the horizontal axis shows the mid-span deflection. As can be seen from Fig. 6, the shapes of the load-deflection curves of all ten beams are similar. Before cracking of the bottom concrete in flexure, the load increased linearly with the deflection; after flexural cracking of the concrete, the load still increased nearly linearly with the deflection but at a slightly smaller slope (i.e. stiffness); and after the ultimate load was reached, the load dropped suddenly to a relatively low level, and then the load only showed a very slight decrease with the deflection (can be seen as a plateau).

### 4.2 *Analysis of test results*

The main test results of the beam specimens are listed in Table 4. It can be seen from Table 4 that the ultimate load of a beam which exhibited Crack Pattern II (e.g. V5SMb) is much smaller than that of a beam which exhibited Crack Pattern I (e.g. V5SMa). It is interesting to note that these two distinct crack patterns resulted in a significant difference in the ultimate load of nearly 70 kN. It is suggested that comparing to Crack Pattern II, Crack Pattern I leads to a smaller span-to-height ratio of the analogous arch, thus a higher maximum load transferred by the arch action. Such a mechanism, which dominates the mechanism of transferring the applied loads to the supports in a test beam, is highly

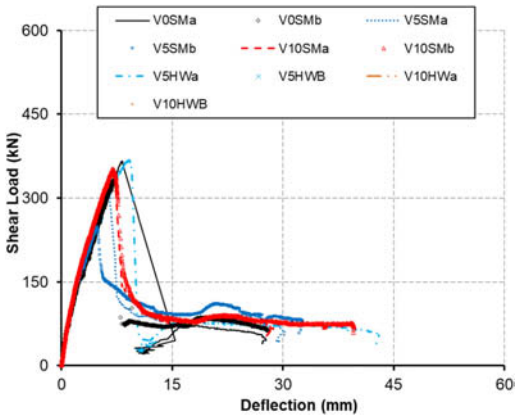


Figure 6. Load-deflection curves of beam specimens.

Table 4. Test results of beam specimens.

| Group | Specimen name | Crack pattern | Ultimate load (kN) | Mean value of ultimate load (kN) | Gain in ultimate load due to FRP needles |
|---|---|---|---|---|---|
| 1 | V0SMa | I | 366 | 350 | - |
| | V0SMb | I | 333 | | |
| 2 | V5SMa | I | 315 | 315* | -10.0% |
| | V5SMb | II | 248 | | |
| 3 | V10SMa | I | 345 | 349 | -0.3% |
| | V10SMb | I | 352 | | |
| 4 | V5HWa | I | 368 | 379 | 8.3% |
| | V5HWb | I | 390 | | |
| 5 | V10HWa | II | 315 | 386* | 10.3% |
| | V10HWb | I | 386 | | |

* Only the beam which exhibited Crack Pattern I was considered.

related to the span-to-depth ratio of the analogous arch as well as concrete compressive strength (Kim and Park 1996). Moreover, it can be seen from Table 4 that replacing coarse aggregate with smooth needles did not increase the shear capacity of the beams (the shear capacity of the beams deceased by 10% when 5% of coarse aggregate in volume was replaced by smooth needles), while replacing coarse aggregate with helically wrapped needles increased the shear capacity of the beam by 8.3%–10.3%. This appears to suggest that the surface type of GFRP needles has a significant effect on the shear capacity of the beam. As can be seen from Fig. 5, for either smooth needles or helically wrapped needles, almost all of the needles were pulled out from the concrete when the width of the main shear crack enlarged, which implies that the bond between the needles and the concrete is critical for the present tests. The volume replacement ratio of coarse aggregate also affects the shear capacity of the beam. For both smooth needles and helically wrapped needles, a larger volume replacement ratio of coarse aggregate

Table 5. Energy absorption of beam specimens.

| Group | Specimen name | Total absorbed energy $E_{total}$ (J) | Mean value of $E_{total}$ (J) | Gain in the $E_{total}$ due to FRP needles |
|---|---|---|---|---|
| 1 | V0SMa | 2108.73 | 2314.07 | - |
| | V0SMb | 2519.40 | | |
| 2 | V5SMa | 2986.98 | 3082.86 | 33.2% |
| | V5SMb | 3178.74 | | |
| 3 | V10SMa | 3235.26 | 3216.32 | 39.0% |
| | V10SMb | 3197.37 | | |
| 4 | V5HWa | 2723.78 | 3208.37 | 38.6% |
| | V5HWb | 3692.95 | | |
| 5 | V10HWa | 2757.75 | 3246.74 | 40.3% |
| | V10HWb | 3735.73 | | |

leads to a larger shear capacity of the beam, but the additional shear capacity gain is not in proportion to the added amount of FRP needles.

### 4.3 *Energy absorption*

The energy absorption of the beam specimens was calculated and listed in Table 5. It should be noted that the calculated total energy is the area under the load vs. mid-span deflection curve when the mid-span deflection is between 0 mm and 27 mm, because the minimum mid-span deflection of the tested beams when the loading was stopped was 27 mm (Specimen V0SMa). It can be seen from Table 5 that the total energy absorbed by the beams with FRP needles is larger than that of the control beams without FRP needles by 33%–40%. With the same volume replacement ratio of coarse aggregate, the beams with helically wrapped needles absorbed more energy than the beams with smooth needles; and with a larger volume of coarse aggregate replaced with either smooth needles or helically wrapped needles, the energy absorbed by the beams increased. Among all the five groups of beams, beams of Group 5 (10% of the coarse aggregate in volume was replaced by helically wrapped needles) absorbed the largest amount of energy. The differences in the sounds made by the beams at failure support this conclusion.

### 4.4 *Discussion*

In terms of the material properties of concrete, including flexural strength, splitting tensile strength and compressive strength, concrete with coarse aggregate replaced with smooth needles performed better than concrete with coarse aggregate replaced with helically wrapped needles. However, in the full-scale specimens replacing the coarse aggregate with smooth needles did not increase the shear capacity of the beam. Replacing the coarse aggregate with helically wrapped needles increased the shear capacity of the full-scale beams by 8%–10%. This implies that the behaviour of large beam specimens with FRP needles is different from the behaviour of small specimens (e.g.

small beams and cylinders) with FRP needles, due to a size effect. The bond behaviour between the FRP needles and the concrete appears to be significant for the shear behaviour of large beam specimens, but not as significant in the small specimens.

## 5 CONCLUDING REMARKS

Cutting FRP waste into FRP needles as coarse aggregate in concrete may be a solution to solve the environmental concern caused by the increasing amount of FRP waste. A total of 10 full-scale RC beams without stirrups in the critical region were tested in the present study. Based on the test results, the following conclusions can be drawn:

1) All test beams failed in shear in a brittle manner with the ductility being slightly enhanced by the partial replacement of coarse aggregate using GFRP needles. Two different crack patterns were observed when the beams failed;
2) An enhancement of 8%–10% in the shear capacity was observed in beams with helically wrapped needles, while beams with smooth needles showed a reduction in the shear capacity. It therefore suggests that bond between FRP needles and concrete plays an important role in the shear behavior of full-scale RC beams;
3) The presence of FRP needles significantly increased the total energy absorbed by the beams by 33%–40%;
4) The test results of the beam specimens do not agree with the findings from the small material test specimens, due to a size effect. The bond behaviour between FRP needles and concrete appears to be critical for the shear behaviour of large beam specimens, but not in the small specimens; and
5) The enhancement of shear capacity of beams by partially replacing the coarse aggregate with GFRP needles adopted in the present study (6 mm in diameter and 100 mm in length) is not remarkable. However, there may be an opportunity to optimize the needles for better performance. The increases in energy absorption and ultimate strength in some beams is an encouraging sign. The influence of shape, size and surface properties of GFRP needles needs to be further examined in future studies.

## ACKNOWLDGEMENTS

The authors gratefully acknowledge the financial support provided by The Hong Kong Polytechnic University (Project account code: 1-BBAG) and Guangdong University of Technology. Partial support for YT and LCB was provided by the US National Science Foundation under grant numbers 1345379, 1551018 and 1701694.

## REFERENCES

ASTM. 2011. Standard test method for tensile properties of fiber reinforced polymer matrix composite bars. *ASTM D7205*. West Conshohocken, PA.

ASTM. 2012. Standard test method for flexural performance of fiber-reinforced concrete (using beam with third-point loading). *ASTM C1609*. West Conshohocken, PA.

ASTM. 2017. Standard test method for splitting tensile strength of cylindrical concrete specimens. *ASTM C496*. West Conshohocken, PA.

ASTM. 2018a. Standard test method for compressive strength of cylindrical concrete specimens. *ASTM C39*. West Conshohocken, PA.

ASTM. 2018b. Standard test method for ignition loss of cured reinforced resins. *ASTM D2584*. West Conshohocken, PA.

BSI. 1987. Method for Tensile Testing of Metals. *BS-18*. London, U.K.

Dong, Z., Wu, G. & Zhu, H. 2019. Mechanical properties of seawater sea-sand concrete reinforced with discrete BFRP-Needles. *Construction and Building Materials*, 206: 432–441.

Kim, J.K. & Park, Y.D. 1996. Prediction of shear strength of reinforced concrete beams without web reinforcement. *ACI Materials Journal*, 93(3): 213–222.

Yazdanbakhsh, A. & Bank, L.C. 2014. A critical review of research on reuse of mechanically recycled FRP production and end-of-life waste for construction. *Polymers*, 6(6): 1810–1826.

Yazdanbakhsh, A., Bank, L.C., Chen, C. & Tian, Y. 2017. FRP-needles as discrete reinforcement in concrete. *Journal of Materials in Civil Engineering, ASCE*, 29(10): 04017175.

Yazdanbakhsh, A., Bank, L.C., Rieder, K.A., Tian, Y. & Chen, C. 2018. Concrete with discrete slender elements from mechanically recycled wind turbine blades. *Resources, Conservation and Recycling*, 128: 11–21.